University of Birjand

Water Harvesting Research (2025) Vol. 8, No. 2: 339-355

10.22077/jwhr.2026.11000.1201

ORIGINAL ARTICLE

Impact of Climate Change on River Discharge and Groundwater Level Using Copula Functions (Case Study: Siminehrood River Basin, Iran)

Fahimeh Sharifan[a], Yousef Ramezani[b*], Mahdi Amirabadizadeh[c], Carlo De Michele[d]

[a]Ph.D. Graduate, Department of Water Engineering, University of Birjand, Birjand, Iran.
[b]Associate Professor, Department of Water Engineering, University of Birjand, Birjand, Iran.
[c]Associate Professor, Department of Water Engineering, University of Birjand, Birjand, Iran.
[d]Professor, Department of Civil and Environmental Engineering, Politecnico di Milano, Milan, Italy.

[*]Corresponding Author E-mail address: y.ramezani@birjand.ac.ir
Received: 06 October 2025, **Revised**: 13 December 2025, **Accepted**: 25 December 2025

Abstract

The aim of this research is to simulate and predict the groundwater level in the Siminehrood River Basin, which is situated south of Lake Urmia, Iran. This simulation was conducted using copula functions while accounting for changes in river discharge influenced by climate change. A total of 26 large-scale CMIP6 models were utilized in this study. Precipitation data were downscaled and simulated using the LARS WG 7.0 model. Subsequently, precipitation data for both the baseline period (1988-2018) and the future period (2031-2050) were predicted for three scenarios: SSP1-2.6, SSP2-4.5, and SSP5-8.5 through a weighted average method. Following the simulation and prediction of precipitation in the Siminehrood River Basin, copula functions were employed to simulate and predict both river discharge and groundwater levels. Prior to fitting the copula function, correlations between pair of parameters precipitation-river discharge and river discharge-groundwater level were examined using Kendall's tau coefficient; correlation values obtained were 0.43 for precipitation-river discharge and 0.44 for river discharge-groundwater level. After selecting marginal distributions and examining these correlations, ten different copula functions were fitted to each pair of parameters in order to identify the most suitable model among them. The results from predicting precipitation related to climate change indicated that annual precipitation under all three scenarios would decrease compared to the measured precipitation. Annual precipitation reductions were projected to be 5.1 mm, 31.5 mm, and 34.8 mm under the scenarios SSP1-2.6, SSP2-4.5, and SSP5-8.5, respectively. Analysis through copula functions revealed that the Clayton copula provided optimal performance when creating a joint distribution for these pair of parameters during simulation phases concerning river discharge as well as groundwater levels and its accuracy was validated based on evaluation criteria including NSE (Nash-Sutcliffe Efficiency), RMSE (root mean square error), and R^2 (coefficient of determination). Furthermore, it was concluded that reductions in annual precipitation would lead to decreases in annual river discharge ranging from 2.9 m^3/s to 6.6 m^3/s alongside an annual drop in groundwater levels estimated between 0.3 m and 1.5 m.

Keywords: Climate change, Copula functions, Downscaling, Marginal distribution functions, Siminehrood River.

1. Introduction

Three-dimensional atmosphere-ocean general circulation models (AOGCMs) are among the most reliable tools for predicting climate change over future periods. As the impacts of climate change are closely tied to the outputs generated by these models (Chen et al., 2019), enhancing their accuracy is crucial for making more dependable predictions based on findings presented in the Climate Change Sixth Assessment Report (Eyring et al., 2016; Stouffer, 2017). The global significance of climate change necessitated the establishment of the Intergovernmental Panel on Climate

Change (IPCC) in 1988, initiated by the World Meteorological Organization (WMO) and supported by the United Nations Environment Program (UNEP).

The IPCC's mandate encompasses a comprehensive assessment of all facets related to this global phenomenon. Key variables such as precipitation, temperature, and solar radiation serve as primary inputs to natural ecosystems, especially in basin environments, where variations can significantly influence productivity and structural integrity. Water availability within a basin is particularly sensitive and serves as a critical factor concerning climate change from economic, social, and environmental perspectives. Consequently, examining how climate change affects this vital resource is imperative. AOGCMs simulate Earth's evolutionary processes across various locations while integrating interactions between atmospheric conditions, ocean currents, sea ice formation, and terrestrial landscapes. These models effectively describe how these components interact with one another to produce and modify complex climatic variables. As such, they play an essential role in simulating climate dynamics over time and space, which ultimately aids in predicting future climatic scenarios (Su et al., 2016).

In summary, AOGCMs not only provide insights into past climatic behaviors but also project potential future changes under varying greenhouse gas emission scenarios. Their ability to represent intricate feedback mechanisms within Earth's system makes them indispensable tools for understanding potential impacts on water resources, a crucial aspect given ongoing concerns surrounding global water scarcity exacerbated by changing climates.

In recent years, the Coupled Model Intercomparison Project Phase 6 (CMIP6) has released a new set of coordinated climate model simulations aimed at supporting the Sixth Assessment Report (AR6). Assessments from various regional studies have indicated that CMIP6 models exhibit improvements over their predecessors utilized in earlier reports (Rivera and Arnould, 2019; Gusian et al., 2020). These advancements have allowed for a deeper examination of the impacts of climate change on various climatic parameters.

Chu et al., (2017) conducted an analysis of agricultural heat and precipitation resources in northeastern China under two Representative Concentration Pathways (RCPs), specifically RCP4.5 and RCP8.5, over the period from 2005 to 2099. Their results demonstrated several significant trends regarding temperature-precipitation distributions across this region. Notably, they found that while temperature consistently decreases from south to north, an overall increase in temperatures was projected across all areas studied. Under RCP4.5, the annual mean temperature is anticipated to reach approximately 9.67°C while under RCP8.5 this figure rises to about 10.66°C, indicating a pronounced warming trend as emissions escalate.

Consequently, changes in other agricultural heat resources are expected to correlate closely with these rising temperatures. Particularly noteworthy is that the rate of temperature increases towards the late 21st century is significantly more pronounced under the more RCP8.5 scenario. Regarding precipitation trends during growing seasons in northern China, there appears to be an upward trajectory. However, this trend lacks statistical significance and is characterized by high annual variability moving forward into future decades. In eastern regions of China, projections indicate an increase in precipitation levels; conversely, western China is expected to experience reductions in precipitation.

Dunning et al., (2018) conducted an assessment of climate change impacts on rainfall patterns in Africa, specifically focusing on the RCP8.5 emission scenario. Their findings suggest a significant increase in rainfall across North Africa, with an average rise of over 100 mm by the end of the 21st century. The study indicates that while the volume of rainfall occurring on rainy days will increase, there will be a corresponding decrease in the total number of rainy days.

Qin et al., (2021) projected temperature and precipitation changes for northwest China under various Shared Socioeconomic Pathways (SSPs) coupled with Representative Concentration Pathways (RCPs). The study forecasts a rise in the annual mean temperature for the long-term period (2081–2100) under different scenarios by 1.4°C (SSP1-1.9), 1.9°C

(SSP1-2.6), 3.3°C (SSP2-4.5), 5.5°C (SSP3-7.0), 2.7°C (SSP4-3.4), 3.8°C (SSP4-6.0), and 6°C (SSP5-8.5). The study indicates that the increase in annual rainfall in the long term will be substantially greater than in both the near-term (2021–2040) and mid-term (2041–2060). The long-term annual rainfall increase will be 4.1% under the SSP1-1.9 scenario, 13.9% under the SSP1-2.6 scenario, 28.4% under the SSP2-4.5 scenario, 35.2% under the SSP3-7.0 scenario, 6.9% under the SSP4-3.4 scenario, 8.9% under the SSP4-3.4 scenario, 8.9% under the SSP4-6.0 scenario, and 27.3% under the SSP5-8.5 scenario compared to the base period (1995-2014).

Shiru et al., (2022) provided an analysis of climate change impacts on precipitation in East Asia using CMIP6 models. The study indicates that precipitation will vary between -32% and +4% across various models for the years 2021-2060. For period 2061-2100, predicted changes become more severe, with projections suggesting a range from -46.7% to +4.4%. Under the SSP5-8.5 scenario, precipitation changes during 2021-2060 are projected to be between -40% and +6.6%. The CanESM5 model specifically predicts precipitation changes from -8.3% to +6.6%, indicating a potential for more localized impacts.

Gebisa et al., (2023) conducted a comprehensive evaluation of climate change projections for the Baro River Basin using simulations from the CMIP6 models. The results showed that precipitation on an annual scale will increase by 6% under the SSP2-4.5 scenario and 16.46% under the SSP5-8.5 scenario. Also, the average maximum temperature on an annual scale will increase by 1.43°C and 1.81°C under the SSP2-4.5 and SSP5-8.5 scenarios, respectively, and the average minimum temperature on an annual scale is predicted to increase by 1.96°C and 3.11°C under the SSP2-4.5 and SSP5-8.5 scenarios, respectively. Abbas et al., (2022) conducted an assessment of precipitation trends in Pakistan utilizing simulations from the CMIP6 models under SSP1-2.6, SSP2-4.5, SSP3-7.0, and SSP5-8.5 scenarios.

The study showed that summer precipitation will increase compared to winter in most scenarios. Annual precipitation will also increase significantly compared to the baseline period. There is a clear trend showing that precipitation increase as one move from lower-pressure scenarios (like SSP1-2.6) to higher-pressure scenarios (such as SSP5-8.5).

The theory of copulas has emerged as a powerful framework for understanding and modeling the dependence structures among random variables. Introduced by Sklar in 1959, copulas allow researchers to link the margins of univariate distributions to create a comprehensive multivariate distribution. This is particularly useful in fields where understanding the relationship between correlated variables is crucial.

A copula is a mathematical function that links the individual marginal distribution functions of correlated random variables, allowing them to create a joint distribution function. Sklar's theorem states that any multivariate distribution can be represented based on its marginal distributions and a corresponding copula. The flexibility provided by copulas to produce joint distributions has led to the increasing use of this method in various studies. Bai et al., (2020) conducted a comprehensive analysis of groundwater level frequency in the Yarkant River basin, utilizing copula functions to investigate the interrelationships between groundwater levels and various driving factors, including runoff and surface water flow.

Their study was notable for its innovative methodology, which combined data from 16 monitoring wells to assess how different variables influenced groundwater levels. The results indicated that groundwater exploitation had the most pronounced negative impact on groundwater levels. The analysis also revealed that runoff and irrigation rates were inversely related to groundwater levels.

Among the various copula types explored, the Frank copula was identified as providing the best fit. Wable and Jha (2018) evaluated the effect of rainfall on groundwater level in West India using Archimedean copula functions. The results showed that Clayton copula function is the best copula function between the rainfall-groundwater level. They also concluded that the method of copula functions between the aforementioned variable pairs is recommended as the best method in conditions of data scarcity.

You et al., (2018) conducted an analysis of the correlation between groundwater levels

and various controlling factors in the Jinghui Irrigation Area of Central China, employing copula functions on annual time series data. Among various copula functions evaluated, the Frank copula was found to provide a satisfactory description of the correlation between groundwater levels and the controlling factors, which included surface water and precipitation.

Nazeri Tahroudi et al., (2021a) conducted a comprehensive study to analyze groundwater level changes in the Nazloochai Basin, specifically focusing on the sub-basin area of the Tapik Hydrometric Station during the statistical period from 2003 to 2015. In this study employed of meta-heuristic algorithms to determine the optimal two-dimensional copula functions. Among the estimation methods compared, the maximum likelihood method demonstrated best performance, achieving a superiority ratio of 131% over the other algorithms tested. The study highlighted the Gumbel-Hougaard copula as the best copula for the two-dimensional analysis of deficiency signatures related to groundwater levels.

The aim of this study is to create a copula-based probabilistic model to assess the impact of climate change on river discharge and groundwater levels within the Siminehrood River Basin. A key innovation of this research lies in the application of the Intergovernmental Panel on Climate Change (IPCC) Sixth Assessment Report for estimating precipitation. The study employs various Archimedean copula functions, including extreme-value, Farlie-Gumbel-Morgenstern (FGM), and Plackett copulas, to facilitate probabilistic predictions and simulations regarding the effects of climate change on river discharge and groundwater levels in the Siminehrood River Basin. This approach allows for a comprehensive understanding of the interconnectedness of these hydrological variables in response to changing climatic conditions.

2. Materials and Methods

The Siminehrood River Basin, a crucial sub-basin of Lake Urmia, is situated at a geographical coordinate of 46.10° longitude and 36.39° latitude in West Azerbaijan Province, covering an area of approximately 2,090 square kilometers. The river is fed by multiple tributaries as it flows westward through Bukan city before ultimately reaching Lake Urmia.

For this study, daily data on precipitation, river discharge, and groundwater levels within the Siminehrood River Basin were utilized. Precipitation measurements were collected using Dashband Bukan rain gauge station selected based on entropy theory. River discharge values were obtained from the Dashband Bukan hydrometric station, one of the oldest and most comprehensive stations in the area, making it suitable for representing total basin discharge (Nazeri Tahroudi et al., 2019).

Groundwater levels (depth that is defined from the Earth's surface to the water table) were monitored using a Mirabad piezometer; this well was also selected based on entropy theory to accurately reflect groundwater conditions across the entire basin (Nazeri Tahroudi et al., 2019). Data spans two significant periods: a baseline period from 1988 to 2018 and a future period from 2031 to 2050. Specifically, variables such as precipitation (mm), river discharge (m^3/s), and groundwater level (m) will be assessed.

Figure 1 illustrates the geographical locations of both the Dashband Bukan hydrometric station and rain gauge station alongside relevant mapping details. Additionally, statistical characteristics pertaining to parameters are compiled in Table 1.

2.1. Radiative forcing scenarios

The Sixth Assessment Report (AR6) of the Intergovernmental Panel on Climate Change (IPCC) introduces a comprehensive framework for analyzing the interactions between climate change and socio-economic factors through various scenarios that combine Shared Socioeconomic Pathways (SSPs) and greenhouse gas concentration trajectories. These pathways include five distinct socio-economic scenarios: 1- SSP1: Sustainable Development (focused on achieving sustainable development goals). 2- SSP2: Intermediate Policy Development (reflects moderate progress in policy implementation). 3- SSP3: Regional Competitiveness (emphasizes regional disparities and

competitiveness). 4-SSP4: Inequality (highlights issues related to inequality across regions and populations). 5- SSP5: Fossil Fuel Development (centers around aggressive fossil fuel use and high energy consumption). These socio-economic pathways are paired with levels of greenhouse gas radiative forcing, allowing for an examination of how various economic developments could influence climate outcomes under different forcing scenarios.

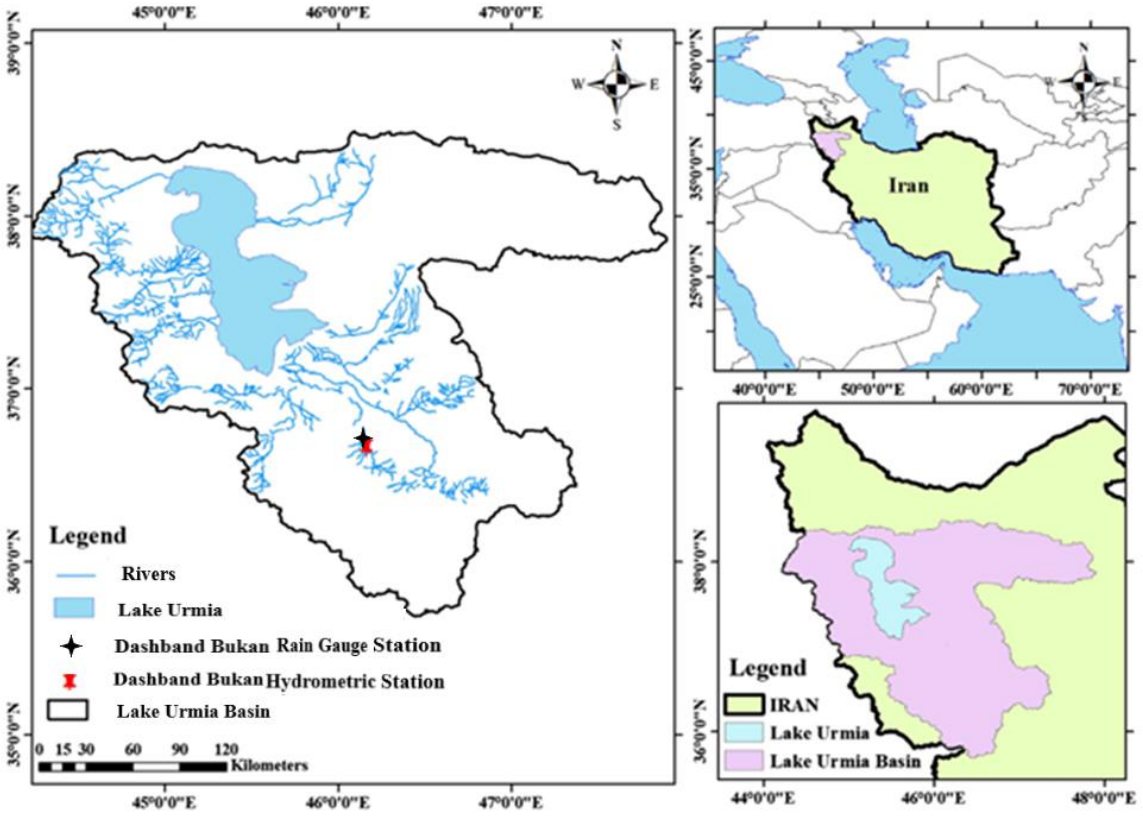

Fig. 1. The geographical location of the Dashband Bukan hydrometric and rain gauge stations

Table 1. Statistical characteristics of the parameters examined on an annual scale

Hydrometric Station	Dashband Bukan
Rain Gauge Station	Dashband Bukan
Piezometer	Mirabad
Average Precipitation (mm)	296.1
Average River Discharge (m^3/s)	17.85
Average Groundwater Levels (m)	5.82
Standard Deviation of Precipitation (mm)	20.3
Standard Deviation of River Discharge (m^3/s)	18.84
Standard Deviation of Groundwater Levels (m)	0.67

In AR6, scenarios are categorized into two groups: Group 1- encompasses range of uncertainties associated with future radiative forcing trajectories critical for climate research, Integrated Assessment Models (IAM), and studies addressing Impacts Adaptation, and Vulnerability (IAV). Baseline scenarios in this group includes: SSP1-2.6: which presents the lowest radiative forcing scenario; SSP2-4.5: indicative of typical socio-economic conditions with intermediate vulnerability; SSP5-8.5: representing a high-end scenario focusing heavily on fossil fuel reliance and elevated energy consumption patterns (Estoque et al., 2020; Rogelj et al., 2018). Group 2- includes hybrid scenarios extend beyond those in Group 1 to capture additional long-term dynamics, including two mitigation-oriented paths aimed at maintaining global average temperature increases below certain thresholds relative to pre-industrial levels, specifically below 1.5 degrees Celsius as well as alternatives involving very high emissions trajectories.

This study employs data from 26 large-scale models presented in the Sixth Assessment Report specifically under three key SSP: SSP1-2.6, SSP2-4.5, and SSP5-8.5 to assess potential impacts relevant to the Siminehrood River Basin in West Azerbaijan Province using

data sourced from the Dashband Bukan meteorological station.

2.2. Downscaling

Unfortunately, general circulation models for local-scale studies have limitations due to their low resolution and large scale, and these models are unable to simulate small-scale climate changes (Wilby et al., 2003). In this research, various methodologies were utilized to downscale precipitation data from GCM models, namely BCSD (Bias Correction and Spatial Disaggregation), SDSM (Statistical Downscaling Model), and the LARS WG 7.0 model. However, because the evaluation criteria for BCSD and SDSM were deemed unsatisfactory, the LARS WG 7.0 model was ultimately chosen for implementation (Sharifan et al., 2025).

After downscaling the models, the evaluation criteria of the coefficient of determination (R^2), Nash-Sutcliffe efficiency (NSE), root mean square error (RMSE), and residual sum coefficient (CRM) were used to select the best models.

$$R^2 = \left[\frac{\sum_{i=1}^{n}(O_i - \bar{O}_i)(p_i - p)}{\sqrt{\sum_{i=1}^{n}(O_i - \bar{O}_i)^2}\sqrt{\sum_{i=1}^{n}\left(p_i - \acute{P}_i\right)^2}}\right] \quad (1)$$

$$NSE = 1 - \frac{\sum_{i=1}^{n}|O_i - p_i|^2}{\sum_{i=1}^{n}|O_i - \bar{O}_i|^2} \quad (2)$$

$$RMSE = \sqrt{\frac{(p_i - O_i)^2}{n}} \quad (3)$$

$$CRM = \frac{\sum_{i=1}^{n} O_i \sum_{i=1}^{n} p_i}{\sum_{i=1}^{n} O_i} \quad (4)$$

In the above equations, $\overline{p_i}$ and $\overline{O_i}$ represent the long-term average of the predicted and measured precipitation in the i-th month, respectively, and n represents the total number of months under study; that is, 12. The most optimal solution for the models will be created when RMSE and CRM tend to zero and R^2 and NSE tend to one.

2.3. Ranking and weighting of models

After evaluating 26 climate models, ranking and weighting of climate models were used to convert the precipitation data into one time series and enter this data into the copula section. After weighting the models, a data series was obtained by multiplying the weights by the model data and calculating their sum for each of the climate scenarios. The weight of each model was obtained using equation 5. In this equation, R_i is the rank of each model in the evaluation index and W_i is the weight of each model (Chen et al., 2011).

$$W_i = \frac{R_i}{\sum_{i=1}^{n} R_i} \quad (5)$$

2.4. Correlation estimation and marginal distribution selection

The application of copula functions in analyzing the relationship between river discharge and groundwater levels involves several structured steps, starting with correlation assessment and moving through marginal distribution fitting, leading to copula selection. To begin, it's essential to assess whether a correlation exists between the pairs of parameters precipitation- river discharge and river discharge- groundwater levels. For this purpose, Kendall's tau coefficient is employed due to its effectiveness in measuring ordinal association without being overly influenced by outliers.

The formula for Kendall's tau coefficient is given by:

$$\tau = \left(\frac{N}{2}\right)\sum_{i<j} sign\left[\left(x_{i-}x_j\right)\left(y_{i-}y_j\right)\right] \quad (6)$$

In Equation 6, N is the number of data, *sign(.)* is the sign function, and x and y are the values of the pair of desired parameters.

Once correlation has been confirmed through Kendall's tau, the next step involves selecting appropriate marginal distributions for each parameter. The goal here is to identify which statistical distribution best fits each dataset.

Two statistical tests are commonly used for this purpose are Kolmogorov-Smirnov and Anderson-Darling tests. Both tests evaluate how well a proposed distribution matches observed data. If the p-values from these tests are significant at the 5% level, can accepted that particular distribution for modeling parameters (Nazeri Tahroudi et al., 2019).

To fit the marginal distributions to the desired parameters, the EasyFit 5.6 model was used, in which the two evaluation criteria mentioned above were used. After confirming the correlation and selecting the best statistical distribution, copula functions can be used.

2.5. Copula functions

Copula functions are mathematical constructs that enable the combination of marginal distributions of various random variables to form a multivariate distribution. The multivariate cumulative distribution function (CDF) can be expressed in terms of its univariate marginal CDFs along with the copula function. A multivariate copula is essentially the joint CDF of standard uniform random variables, capturing the dependence structure between the variables. For a copula $C: [0,1]^2 \rightarrow [0,1]$, it must satisfy specific properties, which are as follows:

Boundary Conditions:

$$C(u,0) = C(0,v) = 0\,, C(1,v) = v\,, C(u,1) = u \quad (7)$$

Associativity Condition:

If $u_1 \geq v_1$ and $u_2 \geq v_2$ and $u_1, u_2, v_1, v_2 \in [0,1]$

$$C(u_1,u_2) + C(v_1,v_2) - C(u_1,u_2) - C(v_1,v_2) \geq 0 \quad (8)$$

Sklar's theorem serves as a fundamental principle in copula theory, stating that any n-dimensional distribution function F can be expressed using a copula C as follows:

$$F(x_1, \dots, x_n) = C(F_1(x_1), \dots, (F_n(x_n)) \quad (9)$$

where $F_1, \dots, F_n$ represent the multivariate distribution functions. If these multivariate distributions are continuous, the copula function C is unique and can be expressed in the following way:

$$(u_1, \dots, u_n) = F\left(F_1^{-1}(u_1), \dots, F_n^{-1}(u_n)\right) \quad (10)$$

where the quantile F_{k-1} is defined as $F_{k-1} = \inf\{x \in R | F_k(x) \geq u_k)\}$. It can also be stated that if C is a copula function and $F_1, \dots, F_n$ are univariate distribution functions, then the function F is an n-dimensional distribution function with margins $F_1, \dots, F_n$. The copulas are divided into different groups such as Archimedean, elliptic and extreme-value, each of these groups includes different copulas.

In the context of bivariate copula modeling, two correlated random variables X and Y are considered, which have respective marginal probability density functions $f_x\left(x; a_1, a_2, \dots, a_p\right)$ and $f_y\,(y; \lambda_1, \lambda_2, \dots, \lambda_r)$. Here, $a_1, a_2, \dots, a_p$ are parameters associated with the distribution of $f_x\,(x)$, and $\lambda_1, \lambda_2, \dots, \lambda_r$ are parameters associated with the distribution of $f_y\,(y)$.

To estimate the parameters from n independent pairs of observations, the log likelihood function for X and Y is $lnL_x\,(x; a_1, a_2, \dots, a_p)$ and $lnL_y\,(y; \lambda_1, \lambda_2, \dots, \lambda_r)$ are maximized individually in order to estimate the parameters.

$a_1, a_2, \dots, a_p$ and $\lambda_1, \lambda_2, \dots, \lambda_r$ are the estimated parameters. The log likelihood function of the joint probability density function of functions $f_{X\,Y}\,(x\,, y)$ is defined as follows:

$$\begin{aligned} &\ln L(x, y; \hat{a_1}, \hat{a_2}, \dots, \hat{a_p}, \hat{\lambda_1}, \hat{\lambda_2}, \dots, \hat{\lambda}, \theta) \\ &= \ln L_c(x, y; F_X(x), F_Y(y), \theta) \\ &+ \ln L_X(\ln L(x; \hat{a_1}, \hat{a_2}, \dots, \hat{a_p}) \\ &+ ln\ L_Y(y; \hat{\lambda_1}, \hat{\lambda_2}, \dots, \hat{\lambda_r}\,) \end{aligned} \quad (11)$$

In equation (11), the log likelihood function of the copula density function is lnL_c. By placing the estimated values for $\lambda_1, \lambda_2, \dots, \lambda_r$ and $a_1, a_2, \dots, a_p$ in equation 5, the log likelihood function lnL to calculate the estimated copula parameter $\widehat{\theta}$ is maximized.

In this research, used of fitting 10 different copula functions to desired pair of parameters, aiming to create a suitable bivariate distribution that first must calculated the correlation between these parameters. To quantify the correlation between the parameters, the Kendall's tau statistic is employed. This non-parametric measure of correlation is particularly useful in the context of copulas. This statistic (equation 11) is used in all studies of copula functions (De Michele and Salvadori, 2003; Nazeri Tahroudi et al., 2022a).

To determine the best copula, the parameters of the copula function are obtained using the IFM method. The optimal copula is then selected by comparing the results of each copula with those of the empirical copula. For a joint two-dimensional copula, the empirical copula of the measured data (u_i, v_i) is defined as follows:

$$C_e(u_i, v_i) = \frac{1}{n}\sum_{i=1}^{n} I\left(\frac{Q_i}{n+1} \leq u_i, \frac{P_i}{n+1} \leq v_i\right) \quad (12)$$

In this equation, C_e is the empirical copula, n is the number of measured data and $I(A)$ is the indicator variable of the logic expression A. If the expression A is true, it will take the value of one and if it is false, it will take the value of zero. Q_i and P_i are the ranks of the i-th

measured data corresponding to the desired pair of copulas.

2.6.Goodness of fit tests for copulas

In this research, Nash-Sutcliffe efficiency (NSE), root mean square error (RMSE) and BIAS evaluation criteria were used to select the best copula function.

$$BIAS = \frac{\sum_{i=1}^{n}(p_i - O_i)}{n} \quad (13)$$

In these equations, $\overline{p_i}$ and $\overline{O_i}$ are the average of the predicted and measured parameters in the i-th month and *n* is the number of data in each parameter, respectively. The best result for the selection of copula functions will be created when BIAS tend to zero.

Table 2. Copula functions used in this research

Family	*C(u,v)*	The domain of $\boldsymbol{\theta}$
Ali-Mikhail-Haq (AMH)	$\frac{uv}{1-\theta(1-u)(1-v)}$	$-1 \le \theta \le 1$
Clayton	$(u^{-\theta}+v^{-\theta}-1)^{-1/\theta}$	$\theta \ge 0$
Frank	$-\frac{1}{\theta}\ln\left[1+\frac{(e^{-\theta u}-1)(e^{-\theta v}-1)}{e^{-\theta}-1}\right]$	$\theta \ne 0$
Galambos	$uv \exp\{[(-lnu)^{-\theta}+(-lnv)^{-\theta}]^{-\frac{1}{\theta}}\}$	$\theta \ge 0$
Gumbel-Hougaard (GH)	$\exp\{-[(-lnu)^{\theta}+(-lnv)^{\theta}]^{\frac{1}{\theta}}\}$	$\theta \ge 1$
Plackett	$\exp\{-[(-lnu)^{\theta}+(-lnv)^{\theta}]^{1/\theta}\}$	$\theta \ge 0$
Farlie-Gumbel-Morgenstern (FGM)	$\frac{1}{2}\frac{1}{\theta-1}\{1+(\theta-1)(u+v)-[(1+(\theta-1)(u+v))^2 - 4\theta(\theta-1)uv]^{\frac{1}{2}}\}$	$-1 \le \theta \le 1$
Gumbel-Barnett (GB)	$uv\,exp\{-\theta(logu)(logv)\}$	$0 < \theta \le 1$
A12	$\frac{1}{1+[(\frac{1}{u}-1)^{\theta}+(\frac{1}{v}-1)^{\theta}]^{1/\theta}}$	$\theta \ge 1$
Joe	$1-[(1-u)^{\theta}+(1-v)^{\theta}-(1-u)^{\theta}(1-v)^{\theta}]^{1/\theta}$	$\theta > 1$

2.7. Joint structure-based simulation

For variable d copula:

$$u_d = C^{-1}_{d|d-1,\dots,1}(w_d|u_{d-1},\dots,u_1) \quad (14)$$

To calculate the conditional distribution function in Equation 15, $C^{-1}_{d|d-1,\dots,1}$ requires a copula pair structure that provides a repetitive expression of h functions for the conditional distribution function (Tahroudi et al., 2020).

The h function for a two-dimensional copula with copula parameter θ_{ij} is defined as follows:

$$h_{i|j} = (u_i|u_j;\theta_{ij}):\frac{\partial}{\partial u_j}C_{ij}(u_i,u_j;\theta_{ij}) \quad (15)$$

$$h_{j|i} = (u_j|u_i;\theta_{ij}):\frac{\partial}{\partial u_i}C_{ij}(u_i,u_j;\theta_{ij}) \quad (16)$$

For simulation and prediction, first a conditional density diagram *c(u,v)* is drawn for one of the desired parameters. In this study, the groundwater level values are simulated under the influence of the desired river discharge values. So, for each river discharge, a diagram u, which is related to the groundwater level, is drawn. Then, the maximum value of *c(u,v)* in each diagram is selected and its corresponding values are calculated on the x-axis.

The maximum values in the drawn diagrams are the groundwater level values that are influenced by the river discharge values (Nazeri Tahroudi et al., 2021b).

3. Results and Discussion

3.1. Evaluation of climate models

As previously stated, 26 GCM models were utilized, included baseline period data from 1988 to 2018 and future period data from 2031 to 2050 for all three scenarios. After the evaluation of the 26 models using criteria such as R^2, NSE, RMSE, and CRM, a ranking of the models was done. The results of this ranking are illustrated in Table 3. It is indicated in this table that the MIROC6 model demonstrated the best performance in simulating precipitation data during the baseline period, aligning with findings by Li et al., (2022) and Tian et al., (2021).

Following the ranking process, weights were assigned to the models. Out of the total of 26 models evaluated, only 6 models (MIROC6, INM-CM5-0, FGOALS-g3, KACE-1-0-G, BCC-CSM2-MR and INM-CM4-8) were given significant weights while nearly zero weight was concluded to the remaining models. For incorporation into the copula section, weights of these 6 models were multiplied by future period data for all three

scenarios (SSP1-2.6, SSP2-4.5 and SSP5-8.5) and thereafter their sum was calculated (Sharifan et al., 2025).

3.2. Assessment of monthly and annual precipitation in the future period

Figures 2 and 3 show the monthly and annual precipitation graphs in the three scenarios SSP1-2.6, SSP2-4.5, and SSP5-8.5.

Figure 2 illustrates that precipitation changes have fluctuations across different months, so that precipitation in some months decreases while others increase.

However, a general trend indicates that in most months, future precipitation under the three scenarios (SSP1-2.6, SSP2-4.5, and SSP5-8.5) will decrease compared to measured historical data. This finding aligns with the research conducted by Abdolalizadeh et al. (2023). Specifically, during the months of May, June, July, and August, as well as September, October, November, December, and January, precipitation shows a decline relative to historical measurements in all three scenarios. Given that significant amounts of precipitation typically will occur in spring, autumn, and winter, it follows that annual precipitation is expected to decrease across all three scenarios, a conclusion supported by Figure 3. Figure 3 reveals that the greatest reduction in precipitation will occur under the pessimistic scenario (SSP5-8.5), while the least reduction related to the optimistic scenario (SSP1-2.6). These results consistent with findings from Ansari et al. (2022).

Table 3. Performance of CMIP6 models for simulating precipitation in the baseline period at the Dashband Bukan synoptic station

Model	R^2	RMSE (mm)	NSE	CRM	Sum of ranks	Final rank
MIROC6	0.86	8.72	0.82	0.1	8	1
INM-CM5-0	0.73	12.18	0.65	-0.12	15	2
FGOALS-g3	0.9	17.81	0.43	-0.61	29	3
KACE-1-0-G	0.4	17.62	0.47	0.11	30	4
BCC-CSM2-MR	0.6	18.51	0.37	0.26	31	5
INM-CM4-8	0.75	19.31	0.33	0.34	32	6
CESM2	0.5	18.48	0.18	0.25	35	7
CMCC-ESM2	0.51	21.16	-0.05	0.27	46	8
MPI-ESM-1-2-HAM	0.42	18.43	0.17	0.45	48	9
E3SM-2-0	0.74	24.02	-0.35	0.41	49	10
MPI-ESM1-2-LR	0.47	22.78	-0.21	0.21	50	11
GISS-E2-1-G	0.5	18.67	0.18	-0.75	52	12
KIOST-ESM	0.55	19.4	0.12	-0.84	55	13
MCM-UA-1-0	0.43	19.04	0.1	-0.82	61	14
CAMS-CSM1-0	0.21	25.42	-0.51	0.12	62	15
GFDL-ESM4	0.88	32.77	-1.6	0.51	63	16
NESM3	0.2	25.98	-0.58	0.09	64	17
MPI-ESM1-2-HR	0.45	29.35	-1.02	0.3	66	18
ACCESS-ESM1-5	0.89	35.00	-1.96	0.54	67	19
MRI-ESM2-0	0.64	34.33	-1.85	0.51	71	20
ACCESS-CM2	0.34	29.52	-1.11	0.38	74	21
NorESM2-LM	0.28	22.51	-0.23	-1.38	75	22
CIESM	0.71	32.26	-1.44	-16	76	23
CanESM5	0.36	25.54	-0.58	-2.8	81	24
IPSL-CM6A-LR	0.52	47.10	-4.37	0.55	82	25
E3SM-1-0	0.5	41.22	-2.98	0.56	84	26

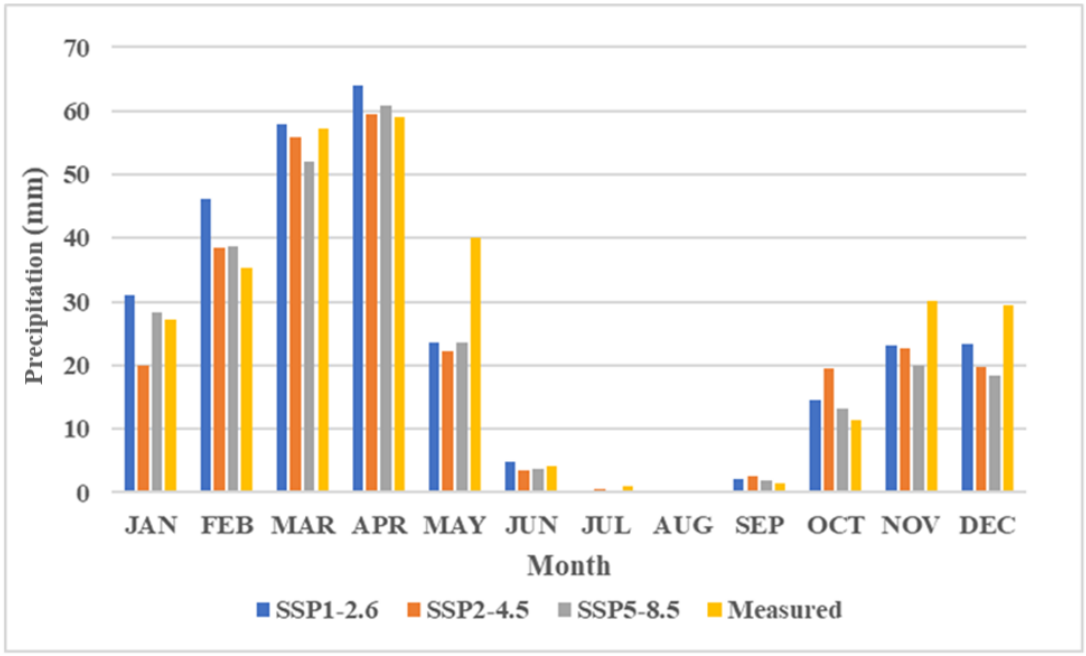

Fig. 2. Comparison of mean monthly precipitation in the baseline period and the future period under the three scenarios

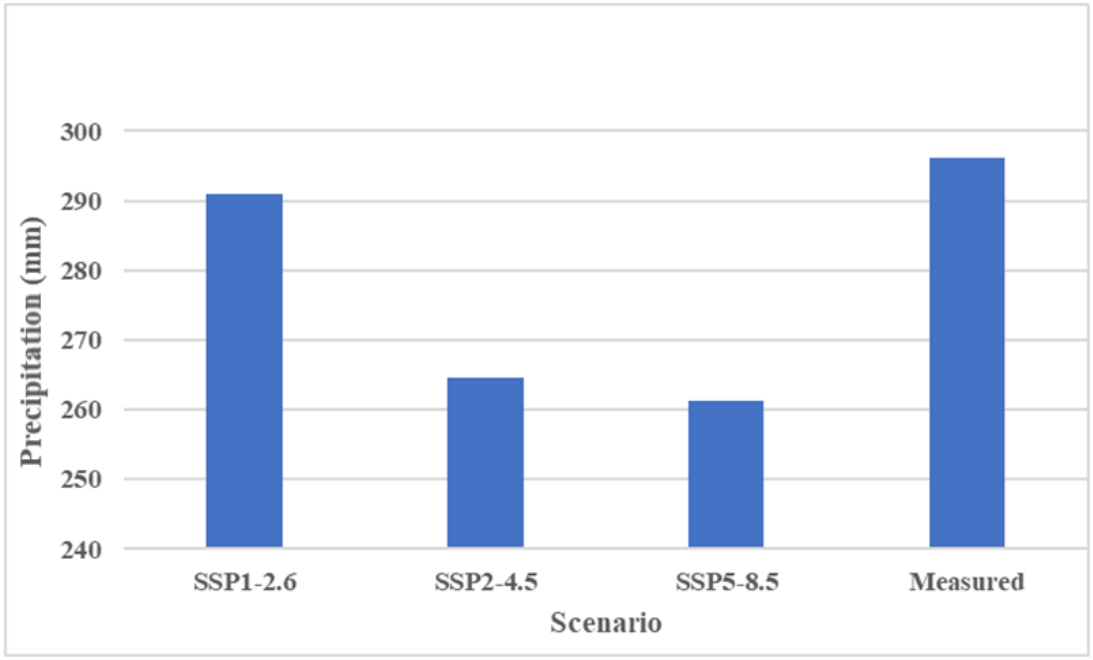

Fig. 3. Comparison of mean annual precipitation in the baseline period and the future period under the three scenarios

3.3. Results of the copula function analysis

Initial steps involved deriving the marginal distribution functions for precipitation, river discharge, and groundwater level parameters using the EasyFit 5.6 software. Subsequently, the correlation between pair of parameters (precipitation-river discharge and river discharge-groundwater level) was investigated through Kendall's tau correlation coefficient. Finally, evaluation criteria were applied to identify the best copula functions. The results yielded from both Kolmogorov-Smirnov and Anderson-Darling tests indicated that precipitation follows a Lognormal distribution, river discharge adheres to a Gamma distribution, and groundwater level aligns with a Lognormal statistical distribution. Furthermore, Kendall's tau correlation coefficients for the pairs of parameters were calculated as 0.43 for precipitation-river discharge and 0.44 for river discharge-groundwater level. These values show an acceptable correlation between each pair.

Previous studies, including those by De Michele and Salvadori (2003), Khashei Siuki et al., (2021), Nazeri Tahroudi et al., (2022), and Dastourani and Nazeri Tahroudi (2022b), have established that correlation values exceeding 0.4 are deemed appropriate for implementing copula-based models. The results pertaining to evaluation criteria aimed at determining the best copula function for these pair of parameters are presented in Tables 4 and 5.

Table 4. Results of goodness-of-fit test of copula functions for precipitation (mm) and river discharge (m^3/s)

Evaluation criteria	AMH	Clayton	Frank	Galambos	GH	Plackett	FGM	GB	A12	Joe
NSE	0.82	0.9	0.53	0.82	0.8	0.84	0.7	0.58	0.82	0.85
RMSE	0.12	0.09	0.19	0.12	0.12	0.11	0.13	0.18	0.12	0.1
BIAS	0.11	0.08	0.18	0.11	0.12	0.1	0.13	0.17	0.11	0.1
Teta	0.99	2.17	-0.91	0.73	1.4	5.23	1	0.1	1	2.08

Table 5. Results of goodness-of-fit test of copula functions for river discharge (m^3/s) and groundwater level (m)

Evaluation criteria	AMH	Clayton	Frank	Galambos	GH	Plackett	FGM	GB	A12	Joe
NSE	0.73	0.94	0.47	0.92	0.82	0.88	0.66	0.43	0.9	0.93
RMSE	0.15	0.07	0.21	0.08	0.12	0.09	0.16	0.21	0.07	0.07
BIAS	0.13	0.06	0.18	0.07	0.11	0.09	0.15	0.19	0.08	0.06
Teta	0.99	6.7	-0.025	20	1.95	20	1	0.1	8.75	7.1

3.4. Simulation and prediction using copula functions

In this section, conditional density of copula functions has been utilized to simulate and predict river discharge and groundwater level parameters, while considering the influence of precipitation. The simulation results for both river discharge and groundwater level are illustrated on daily and monthly scales in Figures 4, 5, and 6.

The simulation process commenced with the modeling of river discharge, which is directly influenced by precipitation. For this purpose, Clayton's copula function employed alongside its conditional density to accurately capture the relationship between these two variables (Sharifan et al., 2024).

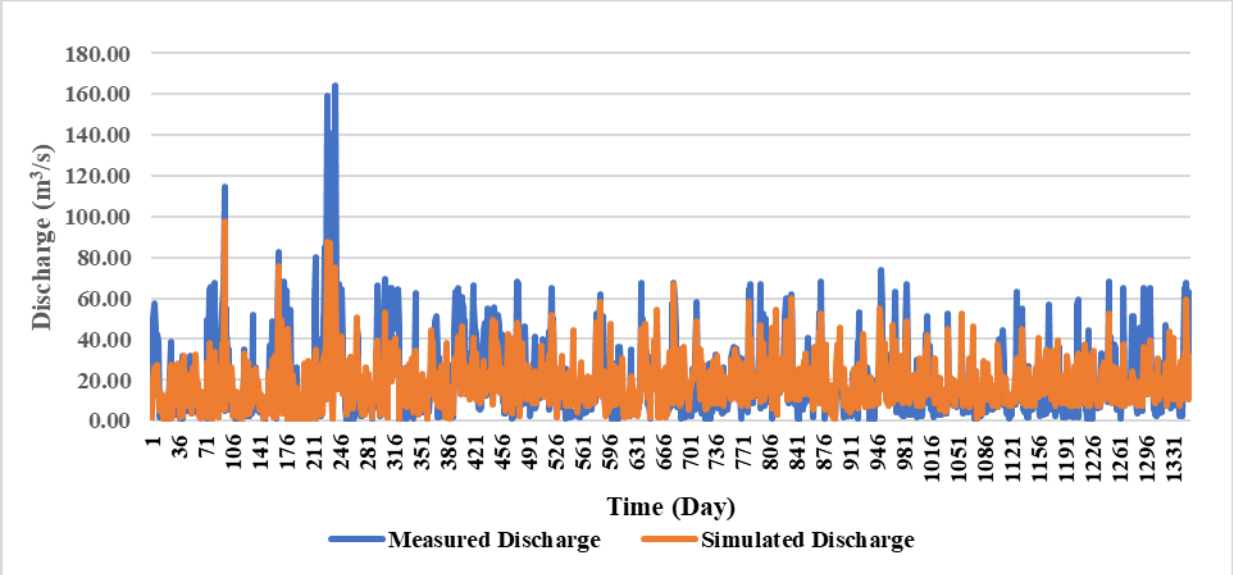

Fig. 4. Simulation of daily river discharge (m^3/s) using Clayton's 2D copula

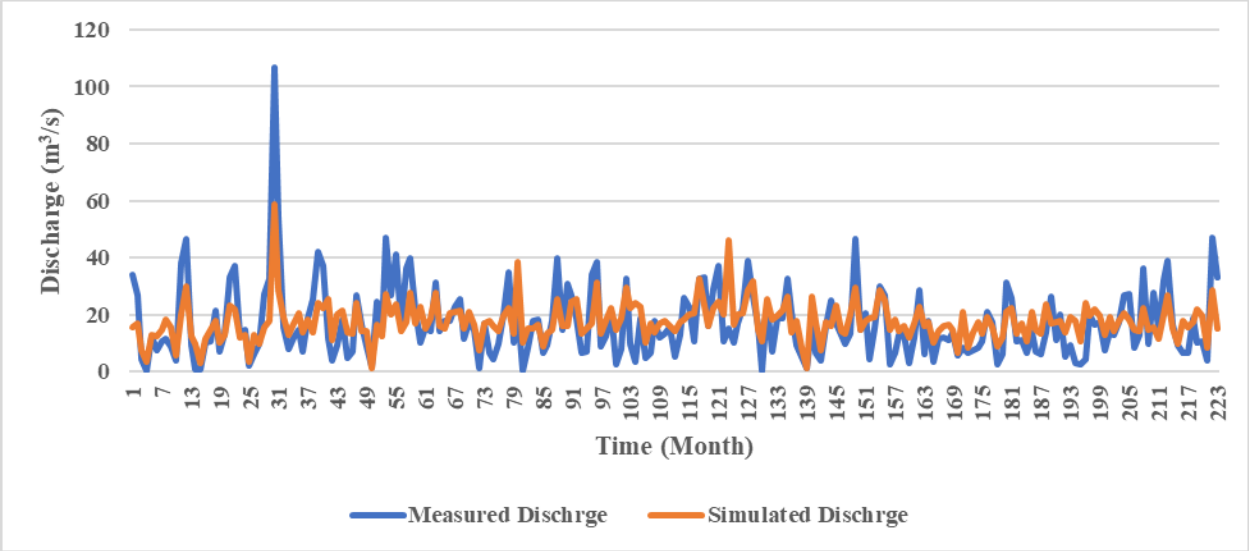

Fig. 5. Simulation of monthly river discharge (m^3/s) using Clayton's 2D copula

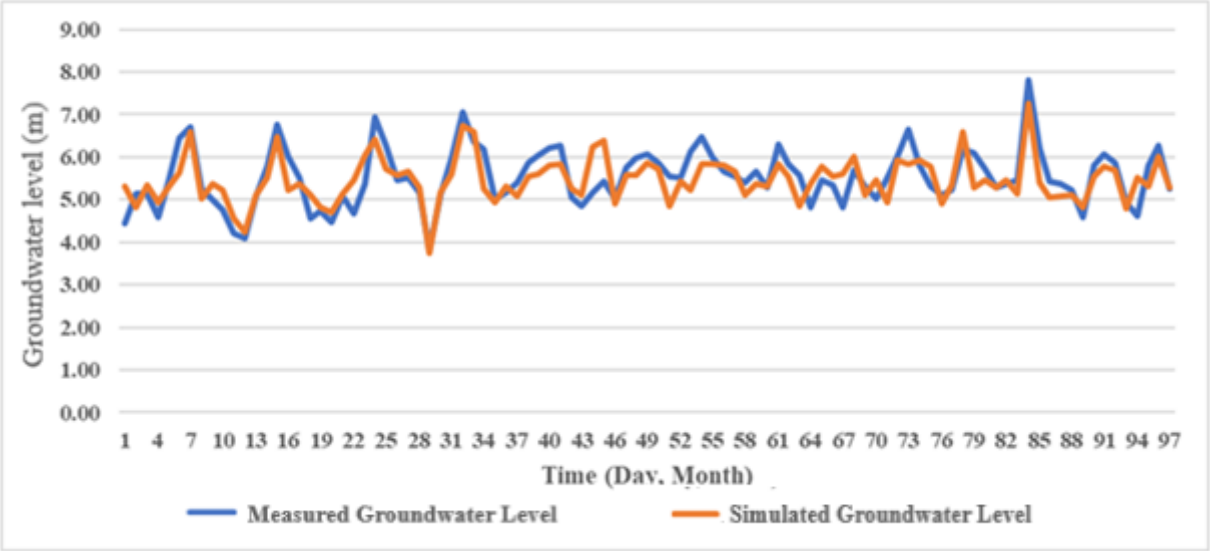

Fig. 6. Simulation of groundwater level (m) using Clayton's 2D copula

According to the simulation graphs, the measured and simulated river discharge and the measured and simulated groundwater level have good correlation on both daily and monthly scales. To estimate the efficiency of Clayton's copula in simulating river discharge and groundwater level, the evaluation criteria of NSE, RMSE, and R^2 were used. The results of the evaluation criteria of river discharge and groundwater level on both daily and monthly scales are given in Tables 6 and 7.

In this study, Tables 6 and 7 have been presented the performance of simulating river discharge and groundwater level. For river discharge, the Nash-Sutcliffe Efficiency (NSE) and R^2 values were calculated at 0.61, and 0.62 on a daily scale, while on a monthly scale these values increased slightly to 0.62, and 0.63, respectively. In comparison, NSE and R^2 values for groundwater level simulation were calculated 0.67, and 0.68, respectively. These coefficients fall within acceptable limits, suggesting that simulations have good efficiency when utilizing Clayton's copula.

Table 6. Evaluation of the efficiency of Clayton's copula in simulating river discharge (m^3/s) on daily and monthly scales

R^2	RMSE (m^3/s)	NSE	Time Scale
0.62	13.18	0.61	Daily
0.63	9.13	0.62	Monthly

Table 7. Evaluation of the efficiency of Clayton's copula in simulating groundwater level (m) on daily and monthly scales

R^2	RMSE (m)	NSE	Time Scale
0.68	0.44	0.67	Daily and Monthly

Furthermore, were assessed simulation accuracy using Root Mean Square Error (RMSE) as an evaluation criterion; results showed RMSE values of 13.18 m^3/s for daily river discharge simulation and 9.13 m^3/s for monthly river discharge assessments and RMSE value was concluded at 0.44 m for groundwater level. Given the range of measured values in both river discharge and groundwater levels, these RMSE confirm choice of Clayton's copula as the best copula. The results highlight that change in groundwater levels are significantly correlated with variations in river discharge over time due to their interdependent relationship within hydrological systems. To account for future conditions influenced by climate change, precipitation data affected by climate variables were incorporated into the simulation equations for predicting future river discharge and groundwater level values were predicted using predicted river discharge under scenarios SSP1-2.6, SSP2-4.5, and SSP5-8.5. The anticipated outcomes from river discharge and groundwater level that covering the period from 2031 to 2050 are depicted in Figures 7 through10 at both monthly and annual scales.

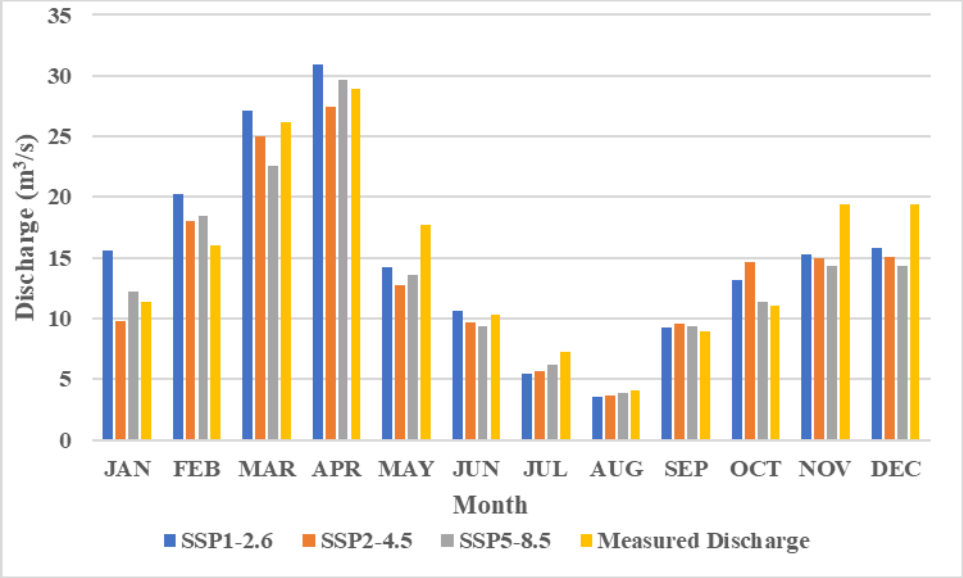

Fig. 7. Prediction of river discharge (m^3/s) under the three scenarios on a monthly scale

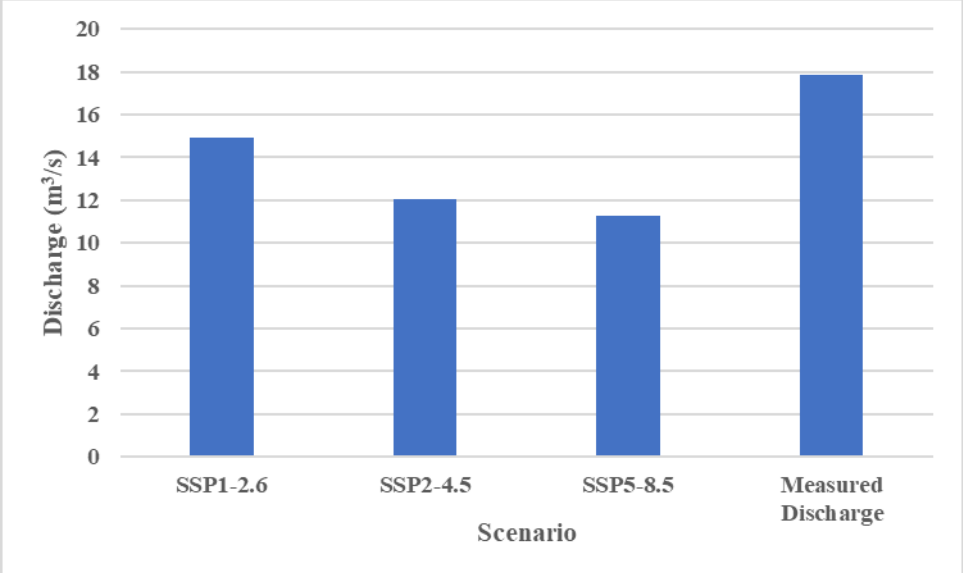

Fig. 8. Prediction of river discharge (m^3/s) under the three scenarios on an annual scale

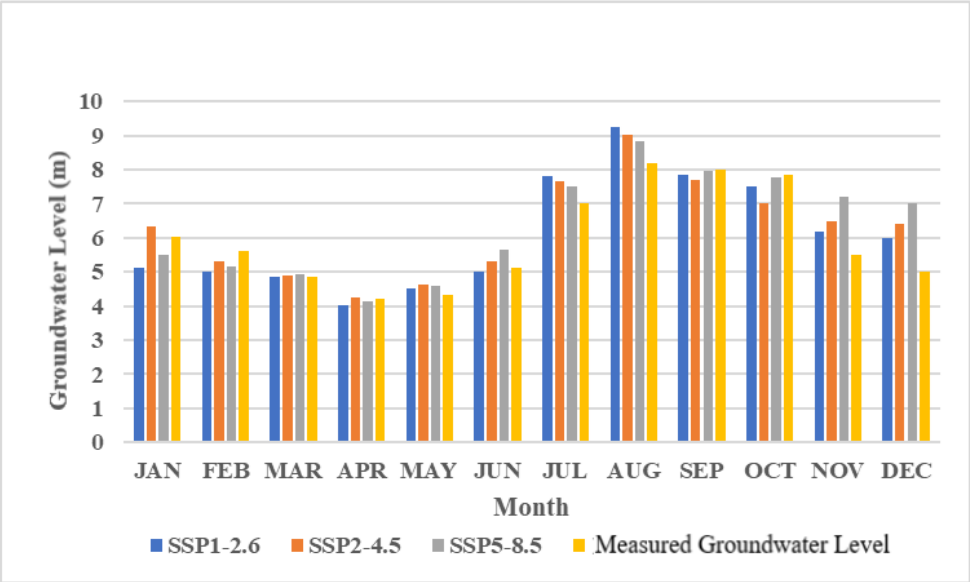

Fig. 9. Prediction of groundwater level (m) under the three scenarios on a monthly scale

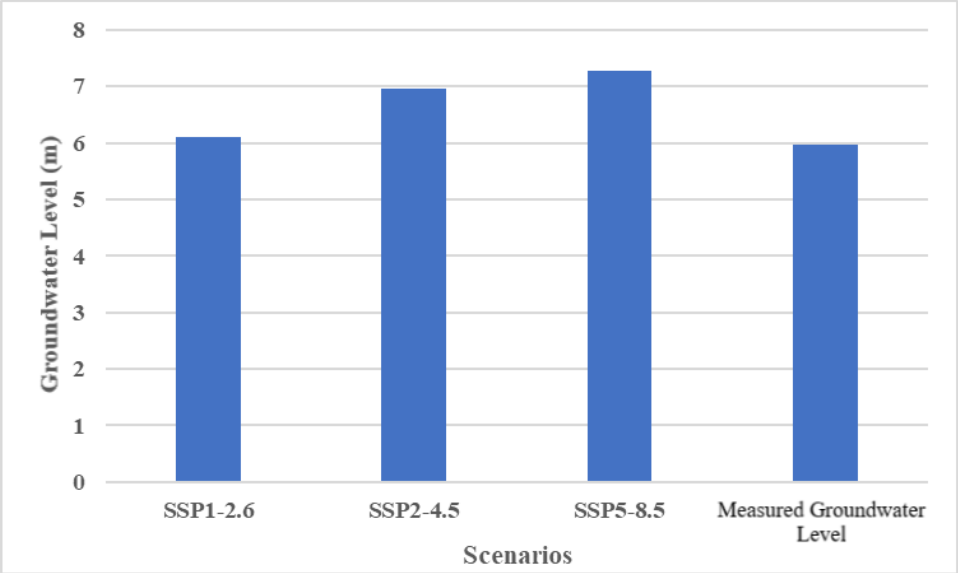

Fig. 10. Prediction of groundwater level (m) under the three scenarios on an annual scale

As can be seen in Figures 7 and 9, fluctuations in river discharge and groundwater levels are anticipated under the considered scenarios considered. In certain months, decreases will be noted, while increases will be recorded in others. It is predicted that the groundwater level drop during May, June, July, August, November, and December will rise across all three scenarios when compared to the measured groundwater levels.

This increase in groundwater level drop is attributed to the decline in river discharge during these months. The decrease in precipitation during this period results in reduced river discharge. In winter and spring seasons, decreases in groundwater level drop will be predict alongside predictions of the highest river discharge.

According to Figures 8 and 10, it is projected that annual drop in groundwater level for the future period will rise across all three scenarios compared to measured values. Additionally, a decline is expected in annual changes concerning river discharge during future period. The predicted values for annual discharge from 2031 to 2050 under the three scenarios (SSP1-2.6, SSP2-4.5, and SSP5-8.5) are estimated at 14.94 m^3/s, 12.02 m^3/s, and 11.24 m^3/s, respectively; while estimates for groundwater levels are forecasted at 6.09 m, 6.95 m, and 7.28 m, respectively. While measured values for both river discharge and groundwater level from the baseline period

have been calculated at 17.85 m³/s and 5.82 m, respectively. The outcomes of simulation regarding Siminehrood River's discharge align with findings presented by Abghari et al. (2023).

4. Conclusion

In the Siminehrood River Basin, the groundwater level is notably close to the earth's surface and shows a significant dependence on recharge from above. This recharge is influenced by both surface water flow and precipitation in the region. This study employs copula functions to simulate and predict the interactions between river discharge and groundwater levels while accounting for climate change impacts. Simulation using copula functions allows the accuracy of the selected copula functions in the analyses to be examined. In this research, copula functions along with their conditional densities, effectively simulated and predicted river discharge and groundwater levels in light of climatic changes affecting the area. The climate change analysis revealed a decline in annual precipitation across all three scenarios (SSP1-2.6, SSP2-4.5, and SSP5-8.5) indicating reductions of 5.1 mm, 31.5 mm, and 34.8 mm, respectively.

This decrease in precipitation is expected to lead to corresponding reductions in river discharge ranging between 2.9 m³/s to as much as 6.6 m³/s annually while simultaneously causing an increase in groundwater level drops estimated at 0.3 m to 1.5 m. Furthermore, correlation analysis using Kendall's tau statistic demonstrated a strong and acceptable relationship between precipitation-river discharge as well as between river discharge-groundwater level in the Siminehrood River Basin, underscoring significant interdependencies among these hydrological factors influenced by climatic change. The study's findings highlight the effectiveness of using copula functions in modeling the hydrological dynamics of the Siminehrood River Basin.

Among various copula functions, the Clayton copula function was identified as the best copula between precipitation-river discharge and river discharge-groundwater level. The simulation results underscore that climate change is expected to induce considerable alterations in both river discharge and groundwater levels by 2050. These significant changes are anticipated to result in severe drinking water shortages in urban areas as well as deficits for agricultural irrigation during dry seasons. By acknowledging the stochastic nature of hydrological phenomena and their interdependencies with various environmental parameters, this study reinforces that copula functions can enhance both analysis and simulation outcomes for hydrological values.

The accuracy demonstrated by the copula-based model during both simulation and prediction phases validates its applicability not only to meteorological and hydrological features but also across different time series data. One notable advantage of using copula functions is their flexibility across diverse geographical contexts. Since these functions focus on modeling statistical distributions rather than being constrained by specific climatic conditions, they maintain robust performance regardless of variations due to latitude, longitude, or other factors impacting data characteristics such as variance, skewness, or extreme value occurrences. This characteristic makes them a valuable tool for researchers aiming to understand complex hydrological systems influenced by varying climatic scenarios globally.

5. Conflict of interest

No potential conflict of interest was reported by the authors.

6. References

Abbas, A., Ullah, S., Ullah, W., Waseem, M., Dou, X., Zhao, C., ... & Ali, G. (2022). Evaluation and projection of precipitation in Pakistan using the Coupled Model Intercomparison Project Phase 6 model simulations. *International Journal of Climatology*, *42*(13), 6665-6684.

Abdolalizadeh, F., Mohammad Khorshiddoust, A., & Jahanbakhsh, S. (2023). Projection of the future outlook of temperature and precipitation in Urmia Lake basin by the CMIP6 models. *Physical Geography Research*, *55*(1), 95-112.

Abghari, H., & Erfanian, M. (2023). Quantifying the Effects of Climate Change on Simineh River Discharge in Lake Urmia Basin. *International Journal of New Findings in Engineering, Science and Technology*, *1*(1), 15-25.

Ansari, S., Dehban, H., Zareian, M., & Farokhnia, A. (2022). Investigation of temperature

and precipitation changes in the Iran's basins in the next 20 years based on the output of CMIP6 model. *Iranian Water Researches Journal*, *16*(1), 11-24.

Bai, Y., Wang, Y., Chen, Y., & Zhang, L. (2020). Probabilistic analysis of the controls on groundwater depth using Copula Functions. *Hydrology Research*, *51*(3), 406-422.

Chen, L., Guo, S., Chen, L., & Guo, S. (2019). Copula-based flood frequency analysis. *Copulas and Its Application in Hydrology and Water Resources*, 39-71.

Chen, W., Jiang. Z., & Li, L. (2011). Probabilistic projections of climate change over China under the SRES A1B scenario using 28 AOGCMs. *Journal of Climate*. *24*(17): 4741-4756.

Chu, Z., Guo, J., & Zhao, J. (2017). Impacts of future climate change on agroclimatic resources in Northeast China. *Journal of Geographical Sciences*, *27*, 1044-1058.

Dastourani, M., & Nazeri Tahroudi, M. (2022). Toward coupling of groundwater drawdown and pumping time in a constant discharge. *Applied Water Science*, *12*(4), 74.

De Michele, C., & Salvadori, G. (2003). A generalized Pareto intensity-duration model of storm rainfall exploiting 2-copulas. *Journal of Geophysical Research: Atmospheres*, *108*(D2).

Dunning, C. M., Black, E., & Allan, R. P. (2018). Later wet seasons with more intense rainfall over Africa under future climate change. *Journal of Climate*, *31*(23), 9719-9738.

Estoque, R. C., Ooba, M., Togawa, T., & Hijioka, Y. (2020). Projected land-use changes in the Shared Socioeconomic Pathways: Insights and implications. *Ambio*, *49*, 1972-1981.

Eyring, V., Bony, S., Meehl, G. A., Senior, C. A., Stevens, B., Stouffer, R. J., & Taylor, K. E. (2016). Overview of the Coupled Model Intercomparison Project Phase 6 (CMIP6) experimental design and organization. *Geoscientific Model Development*, *9*(5), 1937-1958.

Gebisa, B. T., Dibaba, W. T., & Kabeta, A. (2023). Evaluation of historical CMIP6 model simulations and future climate change projections in the Baro River Basin. *Journal of Water and Climate Change*, *14*(8), 2680-2705.

Khashei-Siuki, A., Shahidi, A., Ramezani, Y., & Nazeri Tahroudi, M. (2021). Simulation of potential evapotranspiration values based on vine copula. *Meteorological Applications*, *28*(5), e2027.

Li, X., Fang, G., Wen, X., Xu, M., & Zhang, Y. (2022). Characteristics analysis of drought at multiple spatiotemporal scale and assessment of CMIP6 performance over the Huaihe River Basin. *Journal of Hydrology: Regional Studies*, *41*, 101103.

Nazeri Tahroudi, M., Khashei Siuki, A., & Ramezani, Y. (2019). Redesigning and monitoring groundwater quality and quantity networks by using the entropy theory. *Environmental monitoring and assessment*, *191*, 1-17.

Nazeri Tahroudi, M., Mirabbasi, R., Ramezani, Y., & Ahmadi, F. (2022a). Probabilistic assessment of monthly river discharge using copula and OSVR approaches. *Water Resources Management*, *36*(6), 2027-2043.

Nazeri Tahroudi, M., Ramezani, Y., De Michele, C., & Mirabbasi, R. (2021a). Determination of optimum two-dimensional copula functions in analyzing groundwater changes using meta heuristic algorithms. *Irrigation Sciences and Engineering*, *44*(1), 93-109.

Nazeri Tahroudi, M., Ramezani, Y., De Michele, C., & Mirabbasi, R. (2021b). Flood routing via a copula-based approach. *Hydrology Research*, *52*(6), 1294-1308.

Nazeri Tahroudi, M., Ramezani, Y., De Michele, C., & Mirabbasi, R. (2022b). Application of copula functions for bivariate analysis of rainfall and river flow deficiencies in the Siminehrood River Basin, Iran. *Journal of Hydrologic Engineering*, *27*(11), 05022015.

Nelsen, R. B. (2006). An Introduction to Copulas. Springer, New York. *MR2197664*, 18.

Qin, J., Su, B., Tao, H., Wang, Y., Huang, J., & Jiang, T. (2021). Projection of temperature and precipitation under SSPs-RCPs Scenarios over northwest China. *Frontiers of Earth Science*, *15*, 23-37.

Rivera, J. A., & Arnould, G. (2020). Evaluation of the ability of CMIP6 models to simulate precipitation over Southwestern South America: Climatic features and long-term trends (1901–2014). *Atmospheric Research*, *241*, 104953.

Rogelj, J., Popp, A., Calvin, K. V., Luderer, G., Emmerling, J., Gernaat, D., ... & Tavoni, M. (2018). Scenarios towards limiting global mean temperature increase below 1.5 C. *Nature climate change*, *8*(4), 325-332.

Sharifan F, Ramezani Y, Amirabadizadeh M, De Michele C. (2024). Selection of the Best Copula Function in Bivariate Analysis of Water Resources Components (Case study: Siminehrood River Basin, Iran). *Water Harvesting Research*, *7*(2):289-300.

Sharifan F, Ramezani Y, Amirabadizadeh M, De Michele C. (2025) Evaluating the impact of climate change on precipitation in the future period using CMIP6 models (case study: Siminehrood River Basin, Iran). *Acta Geophysica*, 1-16.

Shiru, M. S., Kim, J. H., & Chung, E. S. (2022). Variations in projections of precipitations of

CMIP6 global climate models under SSP 2–45 and SSP 5–85. *KSCE Journal of Civil Engineering*, *26*(12), 5404-5416.

Sklar, M. (1959). Fonctions de répartition à n dimensions et leurs marges. *Annales de l'ISUP*, *8*(3), 229-231.

Stouffer, R. J., Eyring, V., Meehl, G. A., Bony, S., Senior, C., Stevens, B., & Taylor, K. E. (2017). CMIP5 scientific gaps and recommendations for CMIP6. *Bulletin of the American Meteorological Society*, *98*(1), 95-105.

Su, B., Huang, J., Gemmer, M., Jian, D., Tao, H., Jiang, T., & Zhao, C. (2016). Statistical downscaling of CMIP5 multi-model ensemble for projected changes of climate in the Indus River Basin. *Atmospheric Research*, *178*, 138-149.

Tahroudi, M. N., Ramezani, Y., De Michele, C., & Mirabbasi, R. (2020). Analyzing the conditional behavior of rainfall deficiency and groundwater level deficiency signatures by using copula functions. *Hydrology Research*, *51*(6), 1332-1348.

Tian, J., Zhang, Z., Ahmed, Z., Zhang, L., Su, B., Tao, H., & Jiang, T. (2021). Projections of precipitation over China based on CMIP6 models. *Stochastic Environmental Research and Risk Assessment*, *35*, 831-848.

Wable, P. S., & Jha, M. K. (2018). Application of Archimedean copulas to the impact assessment of hydro-climatic variables in semi-arid aquifers of western India. *Hydrogeology Journal*, *26*(1), 89-108.

Wilby, R. L., Tomlinson, O. J., & Dawson, C. W. (2003). Multi-site simulation of precipitation by conditional resampling. *Climate Research*, *23*(3), 183-194.

You, Q., Liu, Y., & Liu, Z. (2018). Probability analysis of the water table and driving factors using a multidimensional copula function. *Water*, *10*(4), 472.